Registration of Inconsistent Point Cloud Maps with Large Scale Persistent Features

Simon Thompson, Masahi Yokozuka and Naohisa Hashimoto
Smart Mobility Research Group, Robot Innovation Research Center,
National Institute of Advanced Industrial Science and Technology, Tsukuba, Japan

Keywords: Point-Cloud Registration, Inconsistent Maps.

Abstract: Accurate point cloud registration techniques such as Iterative Closest Point matching have been developed to produce large scale 3D maps of the environment. Typically they iteratively register point clouds captured from adjacent sensor scans resulting in point clouds which are largely consistent. However, merging two seperate point cloud maps constructed at different times can lead to significant inconsistencies between the point clouds. Existing point based registration techniques can be sensitive to local minima caused by such inconsistencies. Feature based approaches can overcome local minimum but are typically less accurate, and can still suffer from correspondence errors. We introduce Large Scale Persistent Features (LSPFs), sub regions of point clouds that have orthogonal planar regions that are consistent and persist over a large spatial area. Each LSPF is used to calculate an individual transformation estimate using traditional registration techniques. Sampling Consensus is then used to select the best transform which is used for registration, avoiding local minima. LSPF registration is applied to simulated point cloud maps with known inconsistencies and shown to perform with more accuracy and lower computation time than other popular approaches. In addition, real world registration results are presented which demonstrate LSPF registration between MMS maps and low cost sensor maps captured 6 months apart.

1 INTRODUCTION

Accurate registration of two or more point clouds is required to produce large scale 3D maps of the environment (Pyvanainen et al., 2012)(Shiratori et al., 2015). Point matching based cloud registration techniques, such as Iterative Closest Point (ICP)(Besl and McKay, 1992) typically asumme that point cloud data is captured from spatially *and* temporally close view points, such as consecutive scans of a LIDAR sensor mounted on a moving vehicle (Lu and Milios, 1997). Under this assumption the environment surfaces which the point cloud represents do not drastically change between view points and are generally consistent. However, in some applications, such as merging two seperately constructed maps, the assumption of temporal and spatial proximity in point cloud capture is invalid. In particular, a large temporal distance between point cloud capture can result in significant changes in the environment due to factors such as seasonal variance in vegetation or new construction. This can lead to large inconsistencies (with a non-random distribution) between the point clouds which can cause the registration process to incorrectly converge in local minima. (Thompson et al., 2016) report inconsistencies when merging maps made from low cost sensors (Yokozuka et al., 2015) with high resolution (Tao and Li, 2007) maps captured months apart.

Feature based registration approaches can overcome local minimum but are typically less accurate, can suffer from correspondence errors, and generally require a subsequent fine grained alignment step. This work proposes Large Scale Persistent Features (LSPF) based registration which seeks to overcome local minima problems while still producing the accurate alignment results typical of point cloud matching methods. LSPF are sub regions of point clouds that consist of orthogonal planar regions that persist over a large spatial area. A number of LSPF are detected in the target point cloud and individual alignment is performed on each LSPF and their associated point cloud sub-region. Sampling Consensus is then used to select the registration transform which has the most support. In this way, sub-regions which are inconsistent with the majority of the map can be ignored and local minima in the registration process avoided.

The LSPF registration process is shown to be significantly faster than simple ICP matching, even when

Thompson, S., Yokozuka, M. and Hashimoto, N.
Registration of Inconsistent Point Cloud Maps with Large Scale Persistent Features.
DOI: 10.5220/0006847602740282
In *Proceedings of the 15th International Conference on Informatics in Control, Automation and Robotics (ICINCO 2018) - Volume 2*, pages 274-282
ISBN: 978-989-758-321-6

including the cost of feature detection. Simulation results show that LSPF registration can more accurately register point clouds with inconsistencies than other approaches. Real world registration results are presented which demonstrate LSPF registration between MMS maps and low cost sensor based maps captured 6 months apart.

The rest of the paper is organised as follows: Section 2 describes related work in this field. Section 3 describes LSPFs, how they are detected in point clouds, and how they are used for registration. Section 4 describes a simulated environment with known inconsistencies, and presents registration results evaluating accuracy and computation time for LSPF registration in comparison with other popular approaches. Section 5 then presents some registration results from a real world environment, and also the results from an online data set. Finally Section 6 concludes with some dicussion and introduces avenues for further work.

2 RELATED WORK

The Iterative Closest Point (ICP) algorithm (Besl and McKay, 1992) is a popular technique to align reference and input point clouds in a common frame of reference. In it, corresponding points pairs between the point clouds are indentified by closest Euclidean distance, and then a rigid transformation is calculated which minimises the distance between the corresponding points. The estimated transform is then applied to the input cloud to align it with the reference cloud. This process of first matching corresponding points and then aligning the clouds is repeated until the alignment is sufficiently accurate to meet some convergence criterion.

ICP can produce accurate alignment results but can be sensitive to local minimum in the convergence basin. (Besl and McKay, 1992) state that a global minima can be reached if individual instances of ICP are applied within each local convergence basin, though note the computational challenges this implies. One source of local minimima is due to the interaction between the distribution of points on the underlying surfaces and the choice of correspondence matching metric. Variants of ICP such as Point-to-Plane ICP (Chen and Medioni, 1991), and Generalised ICP (Segal et al., 2009) improve stability and speed of convergence by using more sophisticated matching metrics.

Another, more pernicious source of local minima is inconsistency between the point clouds due to noise in sensor data, or differences in the underlying surfaces. To overcome this, various methods to indentify inconsistent correspondence points have been proposed such as Trimmed ICP (Chetverikov et al., 2002), or RANSAC based correspondence rejection (Holz et al., 2015). In these methods, correspondence points determined to be inconsistent are discarded as outliers before alignment is performed. (Gelfand et al., 2003) propose filtering points based on their stability in the registration task. Only points whose local area covariance matrix suggests good alignment information are used in the registration process. These methods can be computationally expensive and are still susceptible to large non-random inconsistencies.

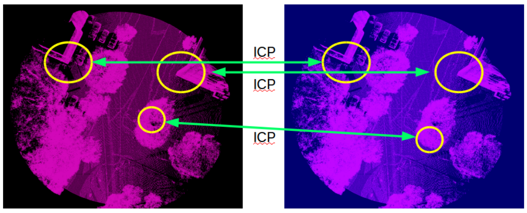

Figure 1: Registration using multiple sub-regions of point clouds.

Feature based registration methods identify key points in the data on which correspondence matching and outlier removal are performed. This reduced correspondence set can be used to calculate a rough initial alignment which avoids local minima. A fine grained point based registration can then applied. (Holz et al., 2015) describe various feature descriptors which encode information at keypoints (Harris and Stephens, 1988) about the local surface curvature and point distribution to improve correspondence matching. FPHF (Rusu et al., 2009) calculate descriptors at different scales to measure persistence of features over spatial extent. Feature descriptor matching however can still suffer from data association errors in both highly structured and unstructured environments.

(Weber et al., 2010) proposes sharp features which use Gauss maps of local surface curvature to identify regions in point clouds with strong peaks in curavture space. This work proposes Large Scale Persistent Features which extend the notion of sharp features to include checking local consistency and persistence over larger regions. Local point cloud sub-regions around features are registered individually using existing point based techniques, avoiding both feature decriptor based correspondence errors and the influence of non-local minima. This idea is illustrated in Figure 1, with multiple sub-regions of the point clouds (shown in cricles) each being aligned individually. Consensus Sampling is then applied to the set of alignment transformations generated by the LSPFs and the most consistent transformation is used to register the point clouds.

3 LARGE SCALE PERSISTENT FEATURES

LSPFs attempt to identify sub regions of the point cloud whose underlying surfaces provide strong cues for registration, and are also likely to be persistent spatially and temporally. It is assumed regions that have mulitple (ideally orthogonal) planar components whose structure remains consistent over a large area satisfy these requirements. LSPF achieve this by analysing the Normal Density Distribution (NDD) of each sampled sub region. Structural consistency over space is determined by the degree to which the NDD of a sub-region remains stable as the size of the region is varied. Strong peaks in the NDD represent planar surfaces and the distance between peaks can determine the relative angle between planar components. Initially a point is randomly sampled from the cloud. This represents the center of a potential LSPF.

3.1 Normal Density Distribution

Given a candidate feature point, the NDD of the surrounding area is calculated. Points within a given radius ($2m$) are randomly sampled. For each of the selected points we use nearest neighbour search to find all points within a radius ($0.3m$) and randomly sample triples of points within. The triples are used to calulate normals (vectors perpendicular to the plane defined by the three points) of the selected points.

Each normal is plotted on a unit sphere to give an Extended Gauss Map of the local surface. The Gauss Map for a candidate feature point on a single planar surface is shown in Figure 2 a). The grey points show the normals on the unit sphere centered on the candidate feature point (large red sphere), with normals concentrated at opposite points on a line perpedicular to the plane. To calculate the density of the normal distribution over the unit shere, we first discretise the sphere using a Fibonnaci Lattice ($N = 10000$). For each point in the Lattice, we then count the number of normals which lie within a given radius, giving the normal density distribution of the candidate LSPF. Figures 2 b) and c) show the NDD for features containing one and two planar surfaces respectively. Red points show the whole point cloud map, green points lie within the radius of the candidate LSPF, while the NDD is drawn on the unit sphere centered on the LSPF, with dark regions being more dense.

3.2 Centering of LSPFs

Because it is assumed persistent features maintain a consistent NDD while varying the size of the feature, surface discontinues (edges or corners) must be centered within the LSPF. To achieve this, when sampling normals, the distance of the plane defined by the normal to the candidate feature point is calculated. By averaging the resulting vectors, a vector which shifts the center of the feature to the point of maximal surface discontinuity is calculated. Iteratively shifting the feature center by this vector (multiped by a gain factor) moves the LSPF to the center of the local surface discontinuities, supressing non-maximal feature detection.

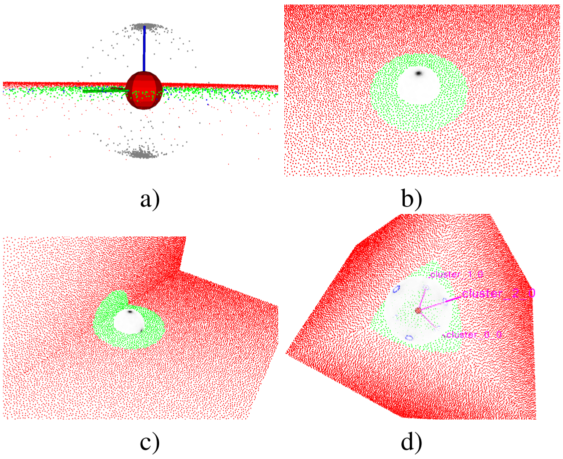

Figure 2: LSPF detection: a) Gauss map of local surface normals, b) Normal Density Distribution (NDD) for one and c) two planes, and d) NDD clustering for corner of a cube.

3.3 Growing Feature Regions

Once a feature is centered, the area covered by the feature is grown to test the persistence of the feature over space. By comparing the evolution of the NDD as the feature region grows, the consistency of the underlying surface structure can be evaluated. In this work we grow the feature radius by $0.2m$ each step, continuously sampling normals from the expanding regions and updating the NDD of the feature. Change in NDD is determined by the Sum of Absolute Differences between the normalised NDD of the initial region and that of the expanded region. When this difference reaches a threshold (experimentally determined), growth is terminated.

3.4 Clustering Normals

Once a LSPF has been centered and grown, the dominant planes in the underlying surface are identified by clustering peaks in the NDD. Using the density of normals discretised by the Fibonacci Lattice, the Density Based Spatial Clustering with Noise (DBSCAN) algorithm is applied. Detected clusters are merged according to the angle between cluster centroids, merging those whose centroids are less than a threshold angular distance apart, as well as clusters lying on opposite sides of the unit sphere. The centroids and density of the remaining clusters form part of the representation of the LSPF. Figure 2 d) shows an example of clusters detected on the corner of a surface with 3 planes.

3.5 LSPF Coverage

Due to the computational expense in caculating LSPFs, an exhaustive evaluation of possible features over the entire point cloud is impractical. Instead, a sampling based approach is used. Random points are iteratively selected and if the point does not lie within the area covered by an existing feature, the above LSPF detection method is applied. A measure of the ratio between points sampled that lead to new features and those that lie within previously identified features, is used as the termination condition of the sampling loop. In this way, sampling continues until 95 percent of sampled points lie within regions covered by LSPF's.

3.6 LSPF Suitability Measure

LSPFs represent persistent spatial structure in the environment. For the registration task, structures with mutiple planar components that extend over a large region are particularly useful. Here, we propose a measure of how suitable a LSPF is for registration based on density and orthogonality of the top three clusters. The ratio of the sum of the density within the top three clusters compared to the total sum of the density over the entire Fibonacci Lattice give an indication of the strength the top three features. Additionally, relatively equal density among the top three clusters represents multiple planar components, while a single dominant density reflects a single plane. Formally, the measure l of the suitability of of LSPF for registration is given by:

$$l = \frac{D(C_1) + D(C_2) + D(C_3)}{\sum_{i=1}^{100} D(fl(i))} * \frac{D(C_1)}{D(C_3)} * \alpha * w_r \quad (1)$$

where, $D(C_j)$ is the density of cluster j, $D(fl(i))$ is the density in the Fibbinoci Lattice i and $w_r o$ is a weight proportional to the radius of the feature. And α represents the orthognality between the cluster centroids:

$$\alpha = (1 - (v_{C_1} \cdot v_{C_2})) * (1 - (v_{C_2} \cdot v_{C_3})) * (1 - (v_{C_3} \cdot v_{C_1})) \quad (2)$$

where v_{C_i} is the centroid vector of cluster i.

3.7 Registration with LSPFs

Given two point clouds (target and input) and an initial guess of the transformation between them, the typical registration task is to calculate the transformation that, when applied to the input cloud, optimally aligns the two point clouds. To perform registration with a set of LSPFs, a transformation estimation algorithm is individually applied to the point cloud defined by each LSPF (all using the same frame of reference and the same initial transformation estimate). For each LSPF, the registration process produces an individual transformation estimate. A sampling consensus algorithm then is applied to chose the transformation estimate with the most support. In this way, LSPFs representing regions of the point clouds which share a common transformation contribute to the registration task, while regions with features which represent inconsistencies can be avoided.

In this work, we apply the well known Iterative Closest Point registration method to estimate transformations between LSPF regions, although any point cloud based method could be used.

4 SIMULATION RESULTS

In this section we present registration results when applying LSPFs to simulated point cloud data, to confirm the ability of the approach to avoid errors in the registration of point cloud data with inconsistencies. A simple, highly structured cloud is used to allow the introduction of inconsistency along the axis of convergence of the registration process. The performance of LSPF registration is compared to that of registration using simple ICP, Point-to-Plane ICP (ICP-PTP), ICP with RANSAC based correspondence rejection, and FPFH feature based Initial Aligment Samping Consensus (IA-SAC) with subsequent fine grained ICP alignment. We use the PCL library (Rusu and Cousins, 2011) for implmentations of all compared methods.

4.1 Simulated Environment

The simulation environment reference point cloud simply consists of a rectangular ground plane with four boxes placed on the ground plane in the four corners, and an additional box in the center. The distribution of cloud data is generated using blue noise sampling over given rectangular planar regions, with noise in the distance to plane applied as well. The resolution of point data is approximately $0.1m$. The input cloud is generated in the same way, with the

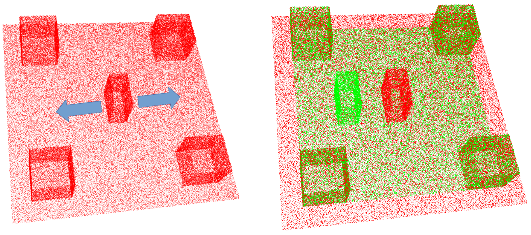

Figure 3: Inconsistency in simulated environment: left) reference map (red), the central object is moved along axis shown by arrows to introduce inconsistencies; right) the reference map overlain with an inconsistent map (green).

central box being shifted along the x axis to produce an inconsistency between the point clouds. The reference ground plane is extended for 2 meters to protect against overlapping errors in the registration task. Figure 3 shows the simulated clouds: a) the reference cloud with arrows showing the axis of the shift applied to the central box; b) the same reference cloud (red), an inconsistent input cloud (green) overlayed on top. Finally an offset is applied to the input cloud to misalign the point clouds for registration.

4.2 Registration with Inconsistencies

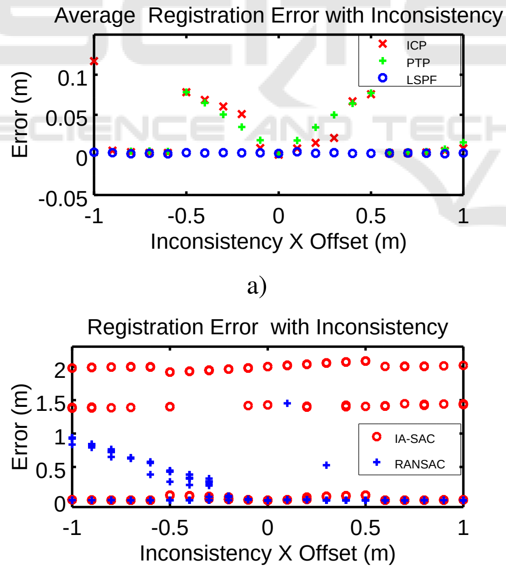

a)

b)

Figure 4: Error in alignment transformation estimate versus distance of point cloud inconsistency: a) average error for LSPF, ICP and ICP-PTP methods; b) error for each trial of RANSAC and IA-SAC methods.

For each trial, simulated reference and input point clouds ($10m \times 10m$) were generated with an inconsistency x_I of $-1.0m$ to $1.0m$ along the x axis in steps of $0.1m$ being introduced to the central box. The entire input cloud was further offset by $1.0m$ on the same axis for misalignment. Experiments were run on machine with an Intel Quad Core i7 64 bit processor.

Table 1: Registration computation time for simulated inconsistent point clouds.

Method	Ave. Comp. Time (S)	(Parallel)
ICP	5.19	
PTP	1.11	
IA-SAC	23.19	
RANSAC	62.75	
LSPF	11.76	(5.05)
LSPF-A	8.07	(3.60)

LSPF detection was applied to the reference cloud and a LSPF set generated. Then, LSPF, ICP, ICP-PTP, RANSAC and IA-SAC registration methods were applied to the misaligned cloud sets, and the estimated transformation and computation time of each method was recorded. For each value of x_I 10 trials were performed. Figure 4 shows the translational error of the estimated alignment transformation for each value of x_I. Figure 4 a) shows the average translational error for each x_I over the 10 trials for LSPF, ICP and ICP-PTP methods. It can be seen that both ICP and ICP-PTP methods have an error proportional to the size of the inconsistency when $-0.5 \geq x_I \leq 0.5$. LSPF, however does not suffer such a decrease in performance.

The plot of error in individual trials in Figure 4 b) shows that the response for RANSAC and IA-SAC methods are multi-modal; that is the registration process converges into different minima depending on randomness within the methods. While IA-SAC does sometimes converge on the true minima (as well as two other distinct minima), the subsequent ICP alignment still suffers the same error as ICP and ICP-PTP as noted above. In comparison, while the RANSAC error is bi-modal, one minima roughly converging onto the value x_I, the other minima converges onto the true alignment, avoiding the errors seen in the ICP and PTP methods.

The average computation time for each method, over all trials, is shown in Table 1. RANSAC and IA-SAC methods are computationally heavy due to sampling and feature detection respectively, while ICP-PTP is the fastest. Computation time for total LSPF and for LSPF alignment only are given. A parallel version of LSPF was also developed and computation times given. One feature of LSPF registration is the ease of parallel processing, as multiple feature detection and subsequent alignment processes can run simultaneously with little synchronisation required.

4.3 Registration with Large Maps

While LSPF is the most accurate, it was shown to be computationally heavy in comparison to ICP-PTP.

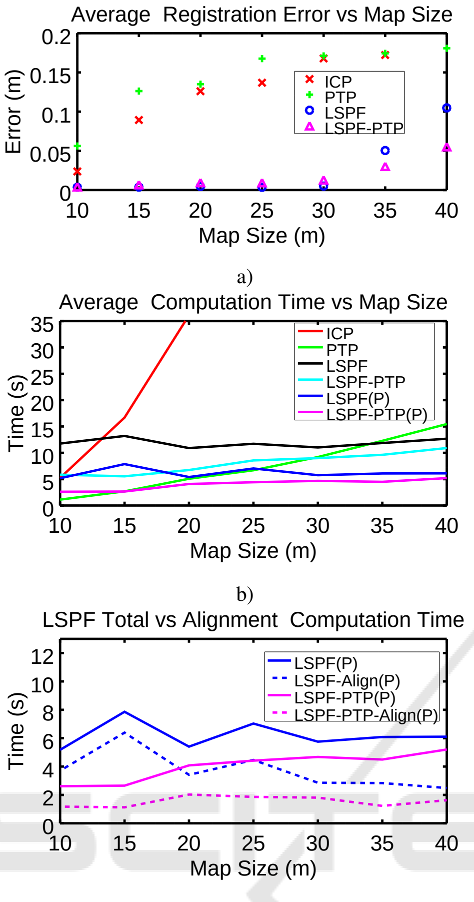

a)

b)

c)

Figure 5: Registration performance for various map sizes: a) Error in estimated transformations for each method, b) Total computation time for each method as well as for parallellised execution of LSPF based methods (P), and c) Total and just alignment computation time for LSPF and LSPF-PTP registration (parallel).

This is because of the cost of feature detection in LSPF and the relatively slow convergence of the ICP algorithm used to align each LSPF region. Because point matching based registration of point clouds tend to increase exponentially with the amount of points in the clouds, it is expected feature based approach such as LSPF will scale better with map size. Here we compare registration accuracy and computation time for LSPF, ICP, ICP-PTP and LSPF-PTP (LSPF registration using ICP-PTP to align each feature region) for maps with increasing ground plane sizes. The map sizes used and their approximate point cloud size are given in Table 2.

Figure 5 a) shows the translational error of each method for map sizes between $10m \times 10m$ and $40m \times 40m$. The error for ICP and PTP increases linearly with respect to map size. LSPF and LSPF-PTP error remains approximately $1/10^{th}$ of ICP error, until map size 35 when they start to increase, but are still much lower than other methods (LSPF-PTP is less than $1/3^{rd}$ the error at map size 40).

Table 2: Map size and approximate point cloud size. Label column shows how map size is denoted in figures.

Map Size (m×m)	Label	Point Cloud Size
10×10	10	59,000
15×15	15	125,000
20×20	20	213,000
25×25	25	325,000
30×30	30	463,000
35×35	35	622,000
40×40	40	806,000

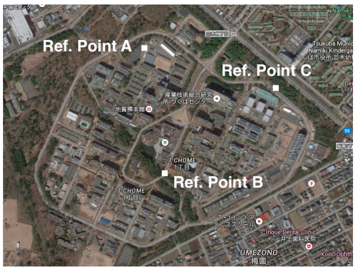

Figure 6: Places of overlap between captured MMS and LCSM maps.

Figure 5 b) shows the average computation time of LSPF, LSPF-PTP (and parallel versions of the two), ICP and ICP-PTP methods for various map sizes. ICP computation time increases exponentially and rapidly rises out of view of the plot. LSPF and LSPF-PTP computation time remains steady even for larger map sizes. ICP-PTP computation starts of low but rises gradually as map size increases, passing both LSPF and LSPF-PTP. Parallel computation times for LSPF-PTP are about one third ICP-PTP by map size 40. Figure 5 c) shows LSPF total and alignment computation times. Alignment time remains less than one quarter of total time for all map sizes.

5 REAL WORLD RESULTS

In this section we present registration results when applying LSPFs to real world point cloud data and compare the performance with that of point-to-plane ICP registration.

5.1 Real World Environment

A large 3D point cloud map of the AIST Tsukuba Central Campus was constructed using a MMS mapping system. A low cost sensor based mapping system (Yokozuka et al., 2015) captured paths within the same environment, but months apart in time, ha-

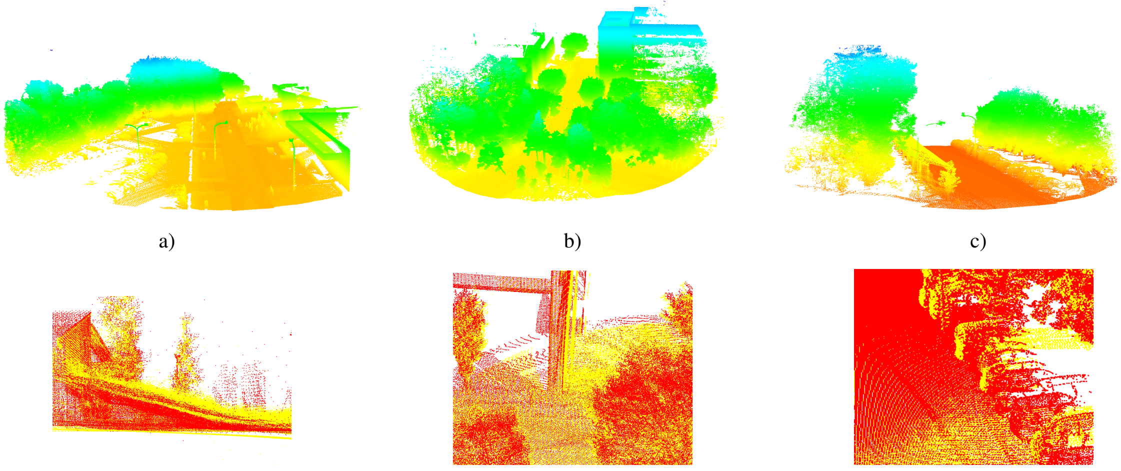

Figure 7: Real world experiment: MMS point clouds for place a) A, b) B and c) C. Inconsistencies between MMS (red) and LCSM (yellow) point clouds: d) vegetation change in place A, e) inconsistent building surfaces in LCSM map in place B, f) parked cars and leafy trees in place C.

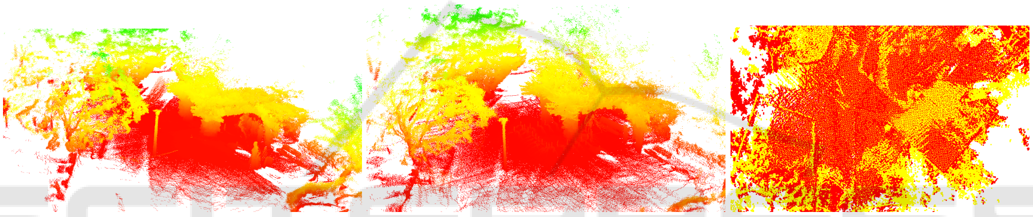

Figure 8: LSPF registration of ASL data sets: a) gazebo in summer, and b) winter, c) the aligned clouds from below.

ving some overlap with the MMS map at three places (see Figure 6). MMS point clouds are accurate and very dense. Here they have been subsampled down to $0.1m$, but still remain approximately double the density than that of the Low Cost Sensor Map (LCSM) clouds. Point clouds taken from the maps at the three reference places are different in environment structure and each have inconsistencies between the MMS and LCSM data (see Figure 7):

- Place A: large open area with car park, vegetation and buildings. Vegetation growth and parked cars provide inconsistencies between clouds.
- Place B: Narrower road, with large buildings and many leafy trees. Internal inconsistencies in LCSM on building faces and ground plane.
- Place C: Narrow road area wisth large leafy trees and parked cars, minimal structured buildings.

Given the structure of the environment it would be expected that registration using LSPF would be most helpful at place A. Indeed, given the structural inconsistencies in buildings in place B, and paucity of persistent built structures in C, we would expect a degradation of performance from A to C.

5.2 Real World Registration

Table 3 shows the map and point cloud sizes for the MMS (reference) and LCSM (input) maps at each of the locations. LSPF detection was performed on the MMS clouds and then LSPF registration was used to align input clouds. Table 4 presents the estimated error in registration for map locations A, B and C, as well as the computation time (total, detection and

Table 3: Real world MMS (Ref.) and LCSM (Input) map and point cloud size.

Map	Radius(m)	Ref. Cloud.	Input Cloud
A	50	1,812,000	1,016,000
B	50	4,447,000	4,442,000
C	25	619,000	194,000

Table 4: Real world MMS and LCSM registration results.

Map	Method	Time(s)[Det., Align]	Err(m)
A	PTP-ICP	113.73	0.1424
	LSPF-PTP	50.71 [45.55, 5.16]	0.0308
B	PTP-ICP	207.47	0.1504
	LSPF-PTP	55.99 [46.98, 9.01]	0.0336
C	PTP-ICP	13.86	0.1201
	LSPF-PTP	21.73 [18.45, 3.28]	0.7575

alignment). For comparison, results using ICP-PTP, the best of the alternative methods in the simulation results, are also presented. Ground truth is assigned by manually aligning point clouds so reported error should be treated with some caution.

Registration in places A and B using LSPFs was both more accurate and required less computation time than PTP-ICP. The presence of structured buildings allows for LSPF based registration to overcome the inconsistencies within the point clouds. The large amount of vegetation however, causes the LSPF detection time to increase, as more features are needed to successfully sample the unstructured elements of the point clouds. Alignment time however is very quick, approximately 5% that of PTP-ICP. Note, LSPF times are using parallel computation.

Registration using LSPF in place C, however, fails to converge on the correct transform. The lack of structured buildings and the large amount of inconsistencies (trees, parked cars), makes it difficult to find features with a consistent registration transform.

5.3 Registration of an Open Data Set

Although many data sets are available to test registration algorithms, they typically consist of data scans captured by moving a vehicle through an environment. ASL (Pomerleau et al., 2012) publish a data set that contains point clouds built from scans captured at different times of the year. The point cloud is of a gazebo covered with vines and surrounding by large trees. The authours describes this as a semi-structured environment with seasonal changes. Example images from a) summer and b) winter point clouds are shown in Figure 8. The initial misalignment between the two point clouds is approximately $1m$.

Here we apply LSPF registration to align the summer and winter data sets. Although no ground truth exists to quantitatively evaluate the alignment, Figure 8 c) shows the aligned clouds from below, where it can be seen that the structured areas of the point clouds such as the corners of the gazebo and the edges of the paths are closely aligned.

6 CONCLUSIONS

This paper presented a method for registration of large scale inconsistent point cloud maps using Large Scale Persistent Features. Feature detection was detailed and a measure for evaluating features for registration based on number and orthogonality of normal density clusters was proposed. Simulated point clouds of structured environments with inconsistent regions were constructed to evaluate registration performance. LSPF registration performance on simulated point clouds was more accurate and faster than other registration techniques for larger point cloud sizes. Real world MMS and LCS maps were merged, with LSPF registration performing better for structured enivironments containing inconsistencies than ICP point-to-plane, although the reverse was true for unstructured environments. This result was expected as LSPFs are specifically designed to detect large structured regions that persist spatially and temporally. LSPF detection time also grows in unstructured environments, as more samples are needed to cover the distribution of unstructured point clouds.

Future work is to apply LSPF to a larger data set of point clouds. Existing data sets tend to have point cloud data captured from spatially and temporally proximal locations, or are limited in extent such as the ASL data set, so a large scale data set with significant inconsistencies between point clouds should be constructed. Also, the LSPF detection process shoud be optimised for speed as for large point clouds detection computation time far exceeds alignment time. Finally, the winner take all consensus sampling within the set of LSPF estimated transforms can lead to incorrect registration in unstructured environments. An approach aggregating a number of transforms might alleviate this problem.

REFERENCES

Besl, P. and McKay, N. (1992). A method for registration of 3-d shapes. In *IEEE Transactions on Pattern Analysis and Machine Intelligence, Vol. 15, No. 2*.

Chen, Y. and Medioni, G. (1991). Object modeling by registration of multiple range images. In *IEEE International Conference on Robotics and Automation*.

Chetverikov, D., Svirko, D., and Stepanov, D. (2002). The trimmed iterative closest point algorithm. In *International Conference on Pattern Recognition*.

Gelfand, N., Ikemoto, L., Rusinkiewicz, S., and Levoy, M. (2003). Geometrically stable sampling for the icp algorithm. In *International Conference on 3D Digital Imagine and Modeling*.

Harris, C. and Stephens, M. (1988). A combined corner and edge detector. In *Fourth Alvey Vision Conference*.

Holz, D., Ichim, A., Tombari, F., Rusu, R., and Behnke, S. (2015). Registration with the point cloud library: A modular framework for aligning in 3-d. In *IEEE Robotics and Automation Magazine, Vol. 22*.

Lu, F. and Milios, E. (1997). Globally consistent range scan alignment for environment mapping. In *Journal Of Autonomous Robots, Vol. 4*.

Pomerleau, F., Liu, M., Colas, F., and Siegwart, R. (2012). Challenging data sets for point cloud registration algorithms. In *International Journal of Robotic Research, Vol. 31, No. 14*.

Pyvanainen, T., Berclaz, J., Korah, T., Hedau, V., Aanjaneya, M., and Grzeszczuk, R. (2012). 3d city modeling from street level data for augmented reality applications. In *In Proceedings of the International Conference on 3D Imaging, Modeling Processing, Visualization and Transmission*.

Rusu, R. B., Blodow, N., and Beetz, M. (2009). Fast point feature histograms (fpfh) for 3d registration. In *IEEE International Conference on Robotics and Automation*.

Rusu, R. B. and Cousins, S. (2011). D is here: Point cloud library (pcl). In *IEEE International Conference on Robotics and Automation*.

Segal, A. V., Haehnel, D., and Thrun, S. (2009). Generalized-icp. In *Robotics: Science and Systems*.

Shiratori, T., Berclaz, J., Harville, M., Shah, C., Li, T., Matsushita, Y., and Shiller, S. (2015). Efficient large-scale point cloud registration using loop closures. In *International Conference on 3D Vision*.

Tao, C. V. and Li, J. (2007). *Advances in Mobile Mapping Technology*. Taylor & Francis Group.

Thompson, S., Yokozuka, M., Hashimoto, N., and Matsumoto, O. (2016). Registration of low cost maps within large scale mms maps. In *IEEE International Conference on Smart City*.

Weber, C., Hahmann, S., and Hagen, H. (2010). Sharp feature detection in point clouds. In *IEEE International Conference on Shape Modeling and Applications*.

Yokozuka, M., Hashimoto, N., and Matsumoto, O. (2015). Low cost 3d mobile mapping system by 6dof localization using embedded sensors. In *International Conference on Vehicular Electronics and Safety*.